The Astrophysical Journal, 627:868–876, 2005 July 10

HIGH-ENERGY EMISSION AND COSMIC RAYS FROM GAMMA-RAY BURSTS

D. Gialis and G. Pelletier[1]
Laboratoire d'Astrophysique de Grenoble, Université Joseph Fourier, BP-53, Grenoble F-38041, France;
denis.gialis@obs.ujf-grenoble.fr, guy.pelletier@obs.ujf-grenoble.fr
Received 2004 May 25; accepted 2005 March 25

ABSTRACT

This paper is devoted to the analysis of particle acceleration in gamma-ray bursts (GRBs) and its radiative consequences. Therefore, we get on one hand constraints on the physics and on the other hand possible signatures of particle acceleration that could be recorded by new gamma-ray instruments. In a recent paper we have shown that UHECRs can be generated in GRBs even with conservative assumptions about the magnetic field and the scattering capability of its perturbations, provided that a suitable relativistic Fermi process is at work during the so-called internal shock phase. In this paper we extend the analysis of the consequences of these assumptions to the whole prompt emission of both electrons and protons. Indeed, assuming that the magnetic field decays as $1/r^2$ and that the scattering time of particles is longer than the Bohm assumption, in particular, with a rule derived from Kolmogorov scaling, we show that the four following events naturally happen with no other parameter adaptation than the intensity of the magnetic field, which turns out to be subequipartition: (1) UHECRs can be generated with a sufficient flux ($\simeq 1$ km^{-2} yr^{-1}) within the GZK sphere to account for the CR spectrum at the ankle. (In the previous paper, we showed that the associated $p\gamma$-neutrino emission is tiny.) (2) A thermal component below the so-called $E_{\rm peak}$ is often unavoidable and even amplified when the shocks start before the photosphere. (3) The CRs could radiate gamma rays around 67 MeV (in the comoving frame, which implies $\simeq$20 GeV for the observer) due to π^0 decay and a low-energy neutrino emission (around 0.2 GeV) associated with neutron decay and also neutrinos of energy between 5 and 150 GeV due to muon decay (as predicted in the previous paper). (4) The UHECRs radiate high-energy gamma rays between a few hundred MeV and 10 GeV (taking the pair creation process into account) due to their synchrotron emission, with a sufficient flux to be observable.

Subject headings: acceleration of particles — cosmic rays — gamma rays: bursts — neutrinos

1. INTRODUCTION

While the afterglow emission of gamma-ray bursts (GRBs) has been well investigated and provided strong support to the "fireball model" (Rees & Mészáros 1992), the origin of the prompt emission is not well established yet. The most widely accepted scenario explaining the burst emission is the internal shock model (Rees & Mészáros 1994): according to this model, the prompt gamma-ray emission results from either the synchrotron emission of accelerated electrons or the inverse Compton scattering off the synchrotron photons, the relativistic electrons being produced by the collision of relativistic shells. But even if the prompt emission spectrum is correctly fitted by the empirical Band function (Band et al. 1993), no physical process satisfactorily explains it, especially below the peak energy ($E_{\rm peak}$). More recently, the possibility of a thermal component as the low-energy part ($\lesssim$100 keV) of the prompt emission spectrum had been studied (Ghirlanda et al. 2003) and successfully compared to observations. In previous papers (Gialis & Pelletier 2003, 2004), we were interested in the issue of the particle acceleration in the internal shocks and in the resulting cosmic-ray generation; our results significantly changed the usual interpretation of the Fermi acceleration (Waxman 1995), and this led us to propose an additional Fermi process to reach the goal of ultrahigh energy cosmic ray (UHECR) production. In this paper, we intend to emphasize the consequences of the particle acceleration on high-energy gamma-ray emission, and we show that the conservative assumptions about the particle acceleration process that allows the generation of UHECRs lead also to a suitable interpretation of the energy spectrum of the prompt emission, except that we do not propose a full understanding of the $E_{\rm peak}$. We also predict both the production of lower energy photons in the UV–X-ray range and a hadronic high-energy emission (between a few hundreds of MeV and 10 GeV, free from opacity effect), which should be detectable, for instance, with the *Gamma-Ray Large Area Space Telescope* (*GLAST*) experiment.

The paper is organized as follows: In § 2, we briefly describe the fireball dynamics from the central object to the deceleration radius. We also calculate the photospheric radius, and we determine some radiative parameters that we need for this paper. Section 3 summarizes our previous results (Gialis & Pelletier 2003) concerning the cosmic-ray acceleration in GRBs and extends the study to the electron population. We analyze the consequences of the particle acceleration on high-energy emission in § 4. The last section of this paper is our conclusion about the new results that we have obtained and which could be confirmed by forthcoming experiments such as High Energy Stereoscopic System 2 (HESS2) and *GLAST*.

2. DYNAMICS AND RADIATIVE PARAMETERS

2.1. *Outline of the Fireball Dynamics*

In this subsection, we briefly summarize all the results we need for this paper that describe the fireball dynamics (Mészáros et al. 1993) before the deceleration radius where an external shock starts. We choose to describe the outflow with a simplified hypothesis: the wind flow can be considered to be a set of discrete shells that are successively emitted with an energy $E_s = E/N_s$, where N_s is the total number of shells and E is the total energy released by the fireball (Daigne & Mochkovitch 1998). We assume

[1] Also at Institut Universitaire de France.

that the total energy radiated in gamma rays, E_γ, is a sizeable fraction of E. According to the observations, this flow is collimated with an average opening solid angle, Ω, of about $4\pi/500$ (Frail et al. 2001). The wind flow duration, namely, Δt_w, happens over an interval of shell number, which is $1 \leq N_s \leq c\Delta t_w/r_0$, where $r_0 \simeq 10^7$ cm is the size of the central object. In a primeval stage of shell expansion, the radiative pressure gives the temperature, T, of the completely optically thick plasma, which is mainly comprised by electron-positron pairs and by electrons and protons beyond the pair annihilation radius. This temperature can initially be defined by

$$T = \left(\frac{3E_s}{4\pi a_s r_0^3}\right)^{1/4}, \tag{1}$$

where E_s is the energy of an emitted shell and $a_s = 7.56 \times 10^{-15}$ (cgs) is the Stefan constant. For an energy E_s on the order of 10^{51} ergs, the temperature at r_0 is about a few MeV.

A characteristic baryon loading parameter, η, is defined as the ratio between E and the baryon rest mass energy:

$$\eta = \frac{E}{M_b c^2} \gg 1, \tag{2}$$

where M_b is the total baryonic mass ejected. The value of the baryon loading parameter is usually considered between 10^2 and 10^3 in order to solve the "compactness problem."

In the first stages, the ejected shell follows an adiabatic expansion in the surrounding medium, and its internal energy is progressively converted into kinetic energy. Hereafter, we define the stationary frame as the rest frame of the central object. In the stationary frame, we can define a radius, r_s, where the kinetic energy of baryonic matter reaches its saturation value. At this moment, the Lorentz factor, Γ, of a given shell is close to η, which constitutes an average value. This last point is important to understand the internal shock model.

In the same frame, the shell thickness, Δr, remains constant and equal to r_0 until the broadening radius $r_b > r_s$ (Goodman 1986; Mészáros et al. 1993). Beyond this radius, the shell thickness becomes $\Delta r \simeq r/2\Gamma^2 \simeq r/\eta^2$, so that the broadening radius is about $\eta^2 r_0$.

In the comoving frame of a shell, entropy and energy conservation inside r_s give the evolution of the Lorentz factor Γ, the temperature T, and the shell thickness, namely, $\Delta R = \Gamma \Delta r$; we have $\Gamma \propto r$, $T \propto r^{-1}$, and $\Delta R = r/r_0$. Thus, the saturation radius r_s is equal to ηr_0.

Beyond r_s, the Lorentz factor Γ remains constant, and the previous evolution laws become $\Gamma \simeq \eta$ and $T \propto r^{-2/3}$. We can also write

$$T \simeq 17\left[\frac{T(r_0)}{5\ \mathrm{MeV}}\right]\left(\frac{\eta}{300}\right)^{-1}\left(\frac{r}{r_s}\right)^{-2/3}\ \mathrm{keV}. \tag{3}$$

Finally, the shell thickness in the comoving frame is such that $\Delta R = \eta r_0$ inside r_b and $\Delta R = r/\eta$ beyond.

The internal shock model has been designed (Mészáros et al. 1993) in order to account for rapid variability observed in GRB light curves, which can reach 1 ms. The internal shock model scheme is as follows: Let us consider two shells leaving the central engine separated by a time interval Δt, respectively, with the Lorentz factors Γ_1 and Γ_2 such that $\Gamma_2 > \Gamma_1$. A collision occurs at the time

$$t_c \simeq \frac{2\Gamma_1^2\Gamma_2^2}{\Gamma_2^2 - \Gamma_1^2}\Delta t. \tag{4}$$

Assuming an instantaneous shock pulse, some time spreading, $\Delta t_s = t_c/2\Gamma^2$, is observed. Thus, the shortest variabilities that are observed ($\sim$1 ms) will be such that $t_b/2\Gamma^2 \simeq r_0/2c$. These correspond to typical timescales associated with the size of a black hole of a few tens of solar masses (namely r_0/c). Such a first collision takes place around the distance r_b. Longer variations correspond to collisions at a more remote distance until they reach a maximum distance determined by the duration of the flow Δt_w. This maximum distance is $r_{\max} \sim r_b c\Delta t_w/r_0$, with $c\Delta t_w/r_0 \simeq 3\times10^3(\Delta t_w/1\ \mathrm{s})$, which gives a proper length of the flow in the comoving frame $\ell_0 = \beta c\Gamma\Delta t_w$. The duration of the flow during the internal shock phase is therefore $\Delta t_{\max} \sim (r_b/r_0)\Delta t_w \sim \eta^2\Delta t_w$. This phenomenon is observed during a time interval shortened by the propagation effect, namely, $\Delta t_{\mathrm{obs}} = (1-\beta)\Delta t_{\max} \simeq \Delta t_{\max}/2\eta^2 \sim \Delta t_w$. The previous value of $r_{\max}$ is not far from the deceleration radius, r_d, of the shells, which is about 10^{16} cm. Also, the Fermi acceleration of particles, which is usually considered (Waxman 1995), takes place in the range that extends from r_b to r_d, namely, the internal shock phase.

2.2. *Radiative Parameters*

We have seen that, in a primeval stage, the ejected plasma is optically thick with respect to the Compton scattering. Using the results of § 2.1, we propose here to determine the photospheric radius, and we define some radiative parameters.

First, it can easily be checked that a typical shell width ΔR becomes smaller than the flow transverse radius after a short while, when $r > \eta(\pi/4\Omega)^{1/2}r_0$, which is comparable to r_s. It will turn out that the photosphere is located at a much larger distance for large enough η, and therefore the opacity of a shell is determined by its width. Assuming the temperature is such that $\bar{\gamma}_e h\nu \ll m_e c^2$, where $\bar{\gamma}_e$ is the average electron Lorentz factor ($\bar{\gamma}_e \simeq 1$ beyond the pair annihilation radius), the optical depth can be defined by $\tau_\star = \sigma_{\mathrm{T}} n_e \Delta R$, where σ_{T} is the Thomson cross section. Because of the plasma neutrality, we have $n_e \simeq n_p$, so that the comoving electron density can be written as

$$n_e = \frac{\xi_s E}{\Gamma\Omega r^2 \Delta R m_p c^2}, \tag{5}$$

where $\xi_s = 1/N_s$. Thus, the optical depth is

$$\tau_\star = \frac{\xi_s \sigma_{\mathrm{T}} E}{\Omega r^2 m_p c^2 \eta}. \tag{6}$$

We can define a critical value for η such that the photospheric radius ($\tau_\star = 1$) is located at r_b, where the particle acceleration at the shocks starts. This critical value $\eta_\star$ is given by

$$\eta_\star \simeq 1780\left(\frac{\xi_s}{10^{-1}}\right)^{1/5}\left(\frac{\Omega/4\pi}{2\times10^{-3}}\right)^{-1/5}\left(\frac{E}{10^{51}\ \mathrm{ergs}}\right)^{1/5}. \tag{7}$$

For a GRB with $N_s \simeq 100$, $\eta_\star \simeq 1100$ and drops around 450 for a long GRB with about 10^4 shells.

Thus, we can express the photospheric radius $r_\star$ as

$$r_\star = r_b\left(\frac{\eta_\star}{\eta}\right)^{5/2}. \tag{8}$$

For usual values of η and according to equation (7), we conclude that the photospheric radius can be larger than r_b, so that the internal shocks start accelerating particles in an optically thick plasma. We analyze some consequences in §§ 3 and 4. Also, beyond $r_\star$, one can consider that photons and electrons decouple and, if $r > r_b$, electrons can be accelerated via the Fermi acceleration in the internal shocks.

Considering the resulting blackbody emission at the photospheric radius, equation (3) gives the temperature, which is such that

$$T_\star = 0.37\left[\frac{T(r_0)}{5\ \mathrm{MeV}}\right]\left(\frac{\eta}{300}\right)^{-5/3}\left(\frac{\eta_\star}{\eta}\right)^{-5/3}\ \mathrm{keV}. \quad (9)$$

This result must be compared to the following one: we have $\chi L_\gamma = \eta^2 \Omega r_\star^2 \sigma T_\star^4$, where χ is defined as the ratio between the average blackbody luminosity, namely, $L_{\rm bb}$, and the GRB gamma-ray luminosity $L_\gamma \lesssim E/\Delta t_w$. We deduce the expression

$$T_\star = 0.47\left(\frac{\chi}{10^{-1}}\right)^{1/4}\left(\frac{\Omega/4\pi}{2\times10^{-3}}\right)^{-1/4} \times\left(\frac{L_\gamma}{10^{51}\ \mathrm{ergs\ s^{-1}}}\right)^{1/4}\left(\frac{\eta}{300}\right)^{-3/2}\left(\frac{\eta_\star}{\eta}\right)^{-5/4}\ \mathrm{keV}. \quad (10)$$

The comparison between equations (9) and (10) leads to a ratio $L_{\rm bb}/L_\gamma$, which easily reaches a few percent:

$$\frac{L_{\rm bb}}{L_\gamma} = 3.8\times10^{-2}\left[\frac{T(r_0)}{5\ \mathrm{MeV}}\right]^4\left(\frac{\Omega/4\pi}{2\times10^{-3}}\right) \times\left(\frac{L_\gamma}{10^{51}\ \mathrm{ergs\ s^{-1}}}\right)^{-1}\left(\frac{\eta}{300}\right)^{-2/3}\left(\frac{\eta_\star}{\eta}\right)^{-5/3}. \quad (11)$$

Thus, the result is a thermal component in the GRB spectrum that can be observed, before higher energy emission, in the range 10–180 keV in the observer frame, as we see in Figure 1. Some authors have already considered this possibility (see, e.g., Ghirlanda et al. 2003), which seems to be consistent with observations. Moreover, we note that equations (9) and (11) indicate a more important thermal component around 100 keV (with $\eta = 400$) for a high number of shells because of a small $\eta_\star$ parameter.

3. PARTICLE ACCELERATION IN THE INTERNAL SHOCK PHASE

3.1. *Proton Acceleration and Cosmic-Ray Generation*

The Fermi acceleration (first or second order) in the internal shock model is usually considered (Waxman 1995) as mildly or subrelativistic with a characteristic time proportional to the Larmor time (Bohm scaling). However, in a previous paper (Gialis & Pelletier 2003), we have shown that this assumption is not realistic regarding the magnetic energy depletion time. Moreover, the Fermi acceleration time depends on the mean free path, $\bar{l}$, of the particle in an irregular magnetic field. This length depends on two other lengths, namely, the Larmor radius, $r_{\rm L}$, and the correlation length, l_c; for a turbulence spectrum of magnetic perturbations in a power law of index β, the following law, which is known in weak turbulence theory, has been extended to the regime of strong turbulence and large rigidities such that $r_{\rm L} < l_c$ (Cassé et al. 2001):

$$\bar{l} = \frac{r_{\rm L}}{\eta_t}\left(\frac{r_{\rm L}}{l_c}\right)^{1-\beta}, \quad (12)$$

where $\eta_t = \langle \delta B^2\rangle/\langle B^2\rangle$. The Bohm scaling $\bar{l} \sim r_{\rm L}$, which holds for electrostatic turbulence, does not apply with purely magnetic irregularities on large scales; no theory or numerical simulation has confirmed Bohm's conjecture. The Bohm estimate corresponds only to the specific case in which the magnetic field is totally disorganized and the Larmor radius is as large as the correlation length, which is not the case in GRBs. The realistic description needs a full analysis of the excitation of MHD turbulence at shocks and its consequence on particle transport. We do not rule out a possible Bohm's scaling upstream of a shock, but the slower scattering process downstream controls the duration of the Fermi cycles. Downstream turbulence is likely governed by a Kolmogorov cascade or its anisotropic version as proposed by Goldreich & Shridar (1995). A forthcoming paper by M. Lemoine et al. (2005, in preparation) will address a full analysis of this issue. In any case, the performance of the Fermi acceleration is very sensitive to the assumption about the scaling of the scattering time. Although we do not claim that this is necessarily so, we reasonably adopt the following assumption: assuming that the correlation length is on the order of a shell thickness, namely, ΔR, the characteristic acceleration time is $t_{\rm acc} = \kappa t_{\rm L}$, where $t_{\rm L}$ is the Larmor time and $\kappa \propto (r_{\rm L}/\Delta R)^{1-\beta}$. According to a Kolmogorov scaling with $\beta = 5/3$ and defining κ_0 as the ratio of the acceleration time over the Larmor time for a Larmor radius that equals the correlation length of the magnetic field, we have

$$t_{\rm acc} \simeq 4.3\times10^{-3}\left(\frac{\kappa_0}{10}\right)\left(\frac{\eta}{300}\right)^{2/3} \times\left[\frac{B(r_b)}{10^4\ \mathrm{G}}\right]^{-1/3}\left(\frac{\epsilon}{1\ \mathrm{GeV}}\right)^{1/3}\left(\frac{r}{r_b}\right)^{(2+\alpha)/3}\ \mathrm{s}, \quad (13)$$

where ϵ is the energy of a proton and the magnetic field strength decreases as $r^{-\alpha}$. Although unproved, this scaling is more reasonable, and this conservative assumption will lead to sensible results. Our main concern is to guarantee UHECR generation with less favorable assumptions than those usually made.

Comparing this time with the expansion time, $t_{\rm exp} = r/c\eta$, we have shown (Gialis & Pelletier 2003) that GRBs are unable to produce UHECRs with this acceleration process because of a strong expansion limitation in energy beyond r_b, which is

$$\epsilon_{\rm exp} \simeq 1.3\times10^4\left(\frac{\kappa_0}{10}\right)^{-3}\left(\frac{\eta}{300}\right)\left[\frac{B_\star(r_b)}{10^4\ \mathrm{G}}\right]\left(\frac{r}{r_b}\right)^{1-\alpha}\ \mathrm{GeV}. \quad (14)$$

This limitation, measured in the comoving frame, is more severe than the synchrotron one and suggests that we have to consider another type of process to achieve high energy. In a recent paper (Gialis & Pelletier 2004), we have proposed a Fermi acceleration process resulting from scattering off relativistic hydromagnetic fronts at the very beginning of the internal shock phase. The efficiency of this process, as shown by numerical simulation, is sufficient to generate a sizeable fraction of UHECRs. In addition, we found that this scenario could constitute a very interesting additional acceleration process that stretches the cosmic-ray distribution tail obtained with the usual Fermi acceleration process. Moreover, in the same spirit, we considered the conservative assumption in which the magnetic field strength decreases like r^{-2} (we also provide formulae with an arbitrary index α); this corresponds to the least favorable situation concerning the particle acceleration. Nevertheless, according to this assumption, we showed that the high-energy cosmic-ray population is such that

$$\frac{dN_\star}{d\gamma} \propto \gamma^{-2}, \quad (15)$$

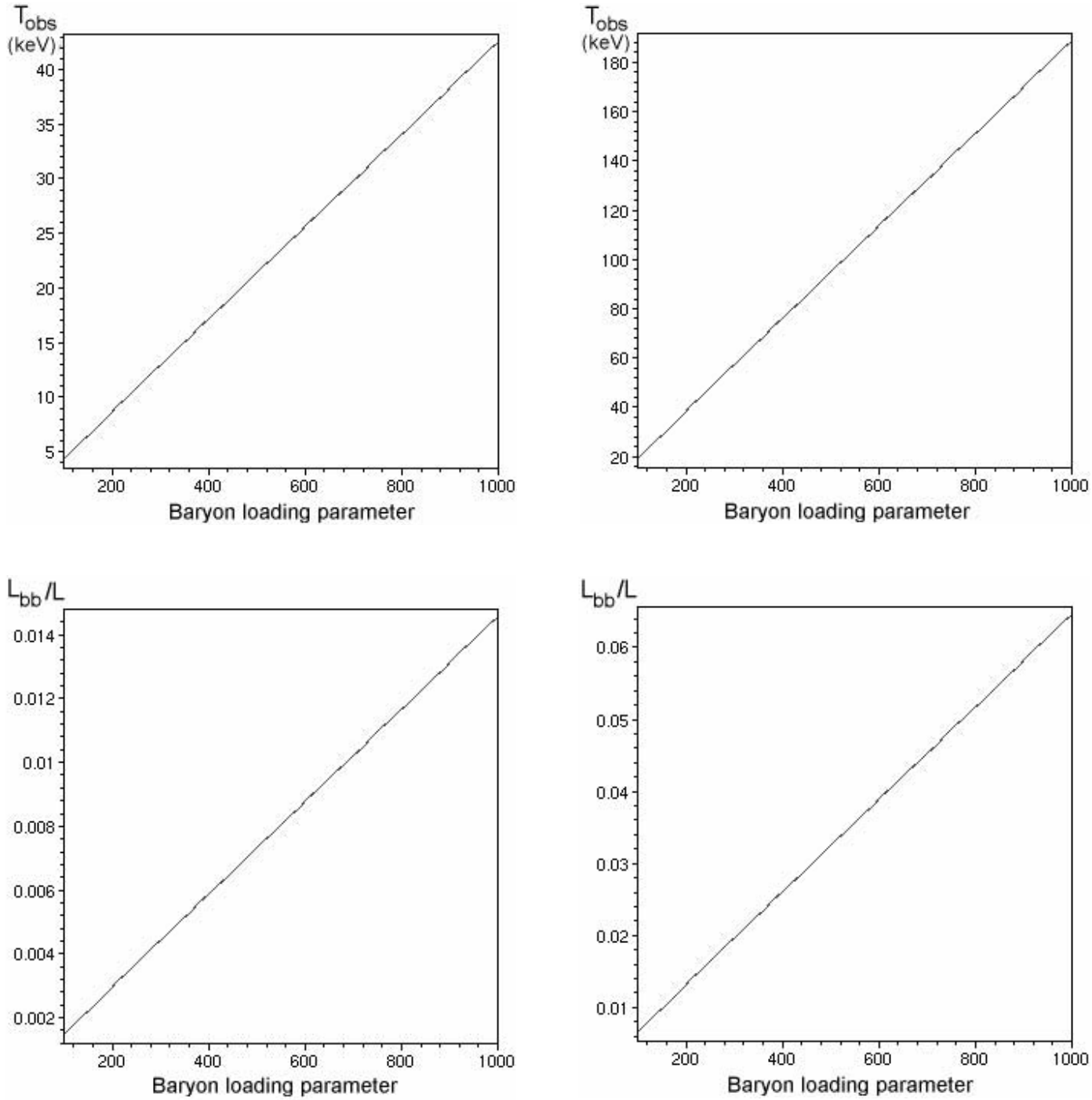

FIG. 1.—*Top*: Variation of the blackbody radiation temperature, measured in the observer frame ($T_{\rm obs} \simeq \eta T_\star$) as a function of the baryon loading parameter η. *Bottom*: Variation of the ratio $L_{\rm bb}/L_\gamma$. *Left*: GRBs with $N_s = 100$ and $\eta_\star = 1100$. *Right*: Long GRBs with $N_s = 10^4$ and $\eta_\star = 450$.

where $N_\star$ is the number of UHECRs and γ is their Lorentz factor; this spectrum extends over 4 decades from 10^7 to 10^{11} GeV in the observer frame.

Assuming such a spectrum for the whole proton population in the comoving Lorentz factor range [1, 10^9], we have

$$\frac{dN_\star}{d\gamma} \simeq N_p \gamma^{-2}, \tag{16}$$

where N_p is the total number of protons released by a GRB. For $N_p \simeq 10^{51}$, the number of UHECRs ($\gamma \geq 10^8$) generated by a GRB is about 10^{43}. Considering a GRB rate of about 1 (10^6 Mpc^{-3} yr^{-1})$^{-1}$ (see, e.g., van Putten & Regimbau [2003] or Frail et al. [2001]), we deduce that, in the Greisen-Zapetin-Kuzmin (GZK) sphere of $\sim$1 Gpc^3, GRBs release 10^{46} UHECRs yr^{-1}. Because of the intergalactic magnetic field, this UHECR population is almost isotropized, so that we can observe $10^{46}/4\pi$ Gpc^{-2} $\sim$ 1 UHECR km^{-2} yr^{-1}, which is about the observed flux at the ankle in the UHECR spectrum. For a better estimate of this flux, we have to consider more accurately the magnetic field structure in the GZK sphere (see, e.g., Lemoine [2003] or Sigl et al. [1999]).

An interesting consequence of the proton acceleration appears in considering the *pp* collisions. Indeed, because $n_p \simeq n_e$, the opacity of *pp* collisions in a shell, namely, $\tau_{pp} = n_p \sigma_{pp} \Delta R$, is

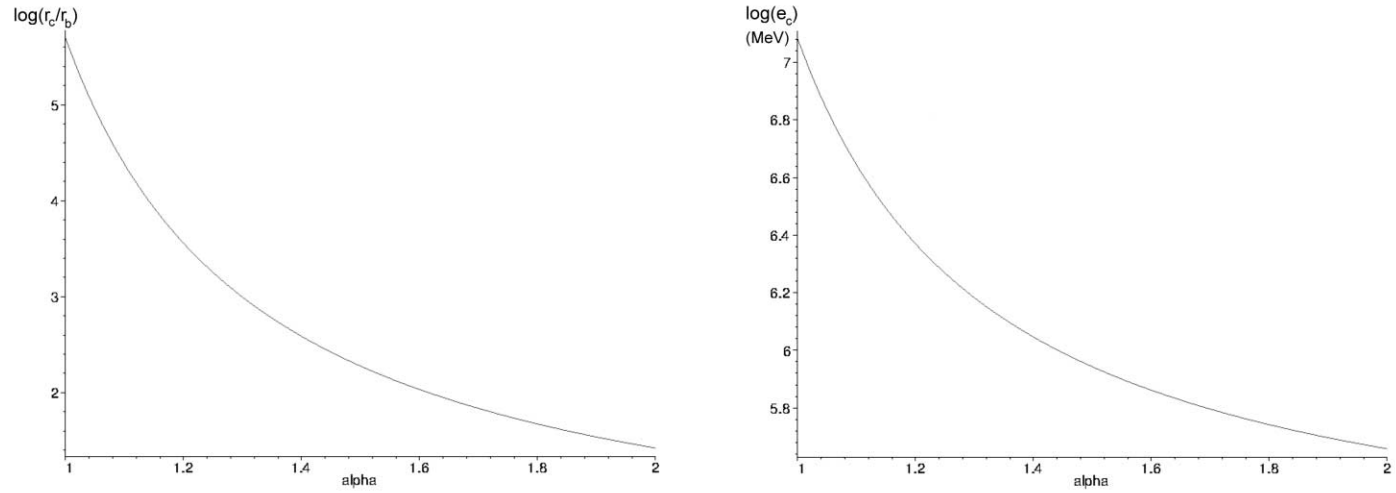

FIG. 2.—*Left*: Variation of r_c/r_b as a function of the magnetic field index α for $\eta = 300$. *Right*: Variation of the cutoff energy ϵ_c.

such that $\tau_{pp} = (\sigma_{pp}/\sigma_{\rm T})\tau_\star$. For this reason, we can easily write the radius r_{pp} beyond which there is no more *pp* collision:

$$r_{pp} = r_\star \sqrt{\sigma_{pp}/\sigma_{\rm T}} \simeq 0.20 r_\star, \tag{17}$$

and $r_{pp} > r_b$ for $\eta < \eta_\star/3$, which is quite possible according to the value of $\eta_\star$ calculated in § 2. (This result slightly differs from that we found in Gialis & Pelletier [2003] because of a better estimate of $\tau_\star$.) In this case, the proton acceleration starts in an opaque stage for *pp* collisions: even if the energy limitation due to *pp* collisions implies a cutoff energy around 1 GeV for the proton population, there is a possibility of a low-energy emission of neutrinos between 5 and 150 GeV, which are produced via the π^+ and the π^- decays (Gialis & Pelletier 2004). Moreover, the *pp* process generates π^0 mesons that decay into photons with an energy of 67 MeV in the comoving frame. Because we have to consider the Klein-Nishina regime, the cross section, namely, $\sigma_{\rm KN}$, is significantly lower than the Thomson cross section ($\sigma_{\rm KN}/\sigma_{\rm T} \simeq 1.7\times10^{-2}$) so that the associated photospheric radius for these photons is about $0.13 r_\star$. The photons produced at 67 MeV in a thin layer between $0.13 r_\star$ and r_{pp} can go through the medium without any electronic interaction; this is achieved if $\eta < \eta_\star/4$. If one considers the pair creation process for 67 MeV photons with themselves, the cross section is such that $\sigma_{\gamma\gamma}/\sigma_{\rm T} \simeq 2.0\times10^{-4}$, which leads to a transparency radius $r_{\gamma\gamma}$ of about $10^{-2} r_\star$ only. Finally, these photons cannot interact with the thermal photons (<0.5 keV) because the threshold energy is about 7.8 keV.

Thus, we predict a possible signature of such a process, which could be observed around 20 GeV in the GRB spectrum when the baryon loading parameter is $\eta < \eta_\star/4$, which mainly occurs for a small number of shells (see eq. [7]). Finally, *pp* collisions also generate a low-energy emission of neutrinos because of the neutron decay that occurs after a proper neutron lifetime of ~13 hr. In fact, the neutron decay produces antineutrinos with energies about 0.7 MeV in the comoving frame. This leads to antineutrinos of 0.2 GeV in the observer frame.

3.2. *Electron Acceleration and Energy Limitation*

In this subsection, we analyze the Fermi acceleration process concerning the electron population, and we use the same formalism as for the proton acceleration. In addition, we assume that electrons and photons decouple at the photospheric radius $r_\star$. Thus, the electron acceleration starts at $r_\star$ if $r_\star > r_b$ and at r_b, otherwise: we can define a radius corresponding to the beginning of the acceleration stage, namely, $r_{\rm acc} = \max(r_\star, r_b)$. In the comoving frame, the acceleration time for an electron with an energy ϵ will be such that

$$t_{\rm acc} \simeq 4.3\times10^{-4} \left(\frac{\kappa_0}{10}\right) \left(\frac{\eta}{300}\right)^{2/3} \times \left[\frac{B(r_b)}{10^4\ {\rm G}}\right]^{-1/3} \left(\frac{\epsilon}{1\ {\rm MeV}}\right)^{1/3} \left(\frac{r}{r_b}\right)^{(2+\alpha)/3} {\rm s}. \tag{18}$$

We deduce that there are two main energy limitations on the electron acceleration beyond $r_{\rm acc}$. The first one is the synchrotron limitation, which is

$$\epsilon_{\rm syn} \simeq 6.5\times10^{2} \left(\frac{\kappa_0}{10}\right)^{-3/4} \left(\frac{\eta}{300}\right)^{-1/2} \times \left[\frac{B(r_b)}{10^4\ {\rm G}}\right]^{-5/4} \left(\frac{r}{r_b}\right)^{(5\alpha-2)/4} {\rm MeV}. \tag{19}$$

The second one is the expansion limitation corresponding to the adiabatic losses:

$$\epsilon_{\rm exp} \simeq 1.2\times10^{7} \left(\frac{\kappa_0}{10}\right)^{-3} \left(\frac{\eta}{300}\right) \left[\frac{B(r_b)}{10^4\ {\rm G}}\right] \left(\frac{r}{r_b}\right)^{1-\alpha} {\rm MeV}. \tag{20}$$

In the comoving frame, we can neglect the dynamical time of an internal shock, which could be written $\Delta t_w/(\eta N_s)$, with $\eta N_s > 10^4$. Thus, at r_b, the synchrotron limitation is the strongest one, but we can define a radius, namely, r_c, where these two limitations are equal and beyond which the main limitation is the expansion one:

$$r_c = \left\{5.4\times10^{-5} \left(\frac{\kappa_0}{10}\right)^{9/4} \left(\frac{\eta}{300}\right)^{-3/2} \left[\frac{B(r_b)}{10^4\ {\rm G}}\right]^{-9/4}\right\}^{4/(6-9\alpha)} r_b. \tag{21}$$

For $\alpha = 2$, $r_c \simeq 26 r_b$, but for α close to 1, this radius is greater than $10^5 r_b$ (see Fig. 2). The electron energy increases and reaches the cutoff energy, ϵ_c, at the radius r_c (see Fig. 3): this energy is

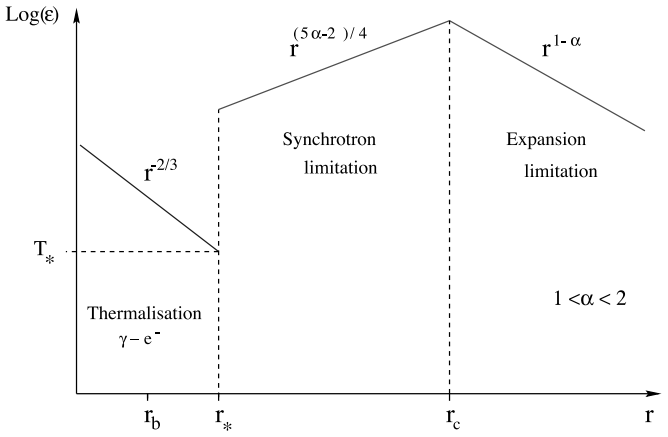

FIG. 3.—Energy limitation in the comoving frame for the electrons. The position of the radius r_c depends on the magnetic field index α and the electron energy at r_c; ϵ_c varies from 10^5 to 10^7 MeV.

very dependent on the magnetic field index α ($B \propto r^{-\alpha}$). We have

$$\epsilon_c \simeq 6.5\times10^2 \left[\left(\frac{\kappa_0}{10}\right)^{6\alpha-3}\left(\frac{\eta}{300}\right)^{(2-5\alpha)/2}\right]^{1/(2-3\alpha)} \times\left\{\left(5.4\times10^{-5}\right)^{5\alpha-2}\left[\frac{B(r_b)}{10^4\ \mathrm{G}}\right]^{-3}\right\}^{1/(6-9\alpha)} \mathrm{MeV}. \quad (22)$$

For $\alpha = 2$, $\epsilon_c \simeq 4.5\times10^5$ MeV, and for α close to 1, this energy reaches 1.2×10^7 MeV.

For an electron with an energy ϵ, the energy near which the synchrotron emission is a maximum can be expressed by

$$h\nu_{\mathrm{syn}} \simeq 7.0\times10^{-4}\left[\frac{B(r_b)}{10^4\ \mathrm{G}}\right]\left(\frac{r}{r_b}\right)^{-\alpha}\left(\frac{\epsilon}{1\ \mathrm{MeV}}\right)^2 \mathrm{eV} \quad (23)$$

and according to equation (19) is on the order of 0.3 keV at r_b, in the comoving frame, for accelerated electrons around the synchrotron energy limit.

Moreover, this energy reaches a maximum value at r_c, and we easily deduce that it is independent of α; indeed, it can be written in the comoving frame as

$$h\nu_c \simeq 2.0\times10^2\left(\frac{\kappa_0}{10}\right)^{-3}\left(\frac{\eta}{300}\right)^{1/3} \mathrm{keV}. \quad (24)$$

As we see in § 4, this energy constitutes a cutoff energy in the high-energy emission spectrum and turns out to be remarkably independent on the magnetic field. Unlike the case of proton acceleration, the additional acceleration by the scattering off the hydromagnetic fronts is not operating because the transit time of the electrons across any shell is too long compared to the synchrotron loss time for an energy above the estimate given by equation (19).

4. CONSEQUENCES FOR HIGH-ENERGY EMISSION

In this section, we focus on the high-energy emission due to both proton and electron populations, and we consider a magnetic field strength that decreases like r^{-2}.

4.1. *Synchrotron Emission by Electrons*

We have seen in § 3 that electron acceleration is limited first by the synchrotron losses and beyond r_c by the expansion losses. We can define the electron energy limitation, namely, ϵ_b, by $\epsilon_b(r) = \epsilon_{\mathrm{syn}}(r)$ up to r_c and $\epsilon_b(r) = \epsilon_{\mathrm{exp}}(r)$ beyond.

According to equations (23) and (24), there is a synchrotron emission over 3 energy decades between 0.3 and 200 keV in the comoving frame, with the highest energy corresponding to the cutoff energy $h\nu_c$. Assuming an electron density, namely, $\rho(\epsilon, r)$, at the distance r and for the energy ϵ such that

$$\rho(\epsilon, r) \propto \epsilon^{-2}\exp[-\epsilon/\epsilon_b(r)], \quad (25)$$

we deduce a local synchrotron spectrum (i.e., depending on the distance r) that can be written as

$$s_e(\nu, r) \propto \int \rho(\epsilon, r)P(\epsilon, r)\delta(\nu - \epsilon^2 g(r))\, d\epsilon, \quad (26)$$

where $P(\epsilon, r) \propto \epsilon^2 g(r)^2$ is the total radiated power for an electron and defining $g(r) = \nu_{\mathrm{syn}}\epsilon^{-2}$, i.e., $g(r) \propto B(r)$ (see eq. [23]). The integration of equation (26) easily gives

$$s_e(\nu, r) \propto g(r)\left[\frac{g(r)}{\nu}\right]^{1/2}\exp\left[-\sqrt{\frac{\nu}{g(r)}}\frac{1}{\epsilon_b(r)}\right]. \quad (27)$$

Moreover, according to equation (23), we can define a local cutoff frequency, namely, $\nu_\star$, by $\nu_\star(r) = g(r)\epsilon_b(r)^2$ so that we have $\nu_\star(r) \propto r^2$ up to r_c and $\nu_\star(r) \propto r^{-4}$ beyond. Thus, the integration over r of equation (27) leads to a time-integrated spectrum:

$$S_e(\nu) \propto \nu^{-1/2} \times\left\{\int_{r_b}^{r_c} r^{-3}\exp\left[-\sqrt{\frac{\nu}{\nu_\star(r_c)}}\frac{r_c}{r}\right] dr + \int_{r_c}^{r_d} r^{-3}\exp\left[-\sqrt{\frac{\nu}{\nu_\star(r_c)}}\frac{r^2}{r_c^2}\right] dr\right\}, \quad (28)$$

where $\nu_\star(r_c)$ corresponding to ν_c is the high cutoff frequency.

Considering the case $\nu < \nu_c$, i.e., around 0.3 keV in the comoving frame, we show in the Appendix that equation (28) could be simplified, and we obtain

$$S_e(\nu) \propto \nu^{-1}. \quad (29)$$

Thus, electrons provide a gamma-ray emission that is composed of a thermal component below 0.3 keV (see § 2.2) and of a synchrotron component above. In the observer frame, the energy separating these two components could constitute the usual E_{peak} (see, e.g., Band et al. 1993), which is the energy for which the gamma-ray emission is the most important (i.e., the peak energy of the burst). However, most of the observations do not clearly exhibit such a ν^2 spectrum in the low-energy range, although the fireball model unavoidably has such a signature. It turns out that the lowest value of the synchrotron cutoff, as displayed by the limitation energy diagram, which corresponds to an emission at r_b, fits with the observational value of E_{peak}. However, we have not yet a clear understanding of the decrease of the synchrotron spectrum at lower energies down to where it meets the blackbody spectrum and especially how it evolves beyond r_b. Moreover, it depends on the baryon loading parameter η, because $E_{\mathrm{peak}} \simeq \eta h\nu_{\mathrm{syn}}(r_b)$, putatively, and can vary from 30 keV to about 300 keV in the observer frame. Despite the lack of clear understanding of E_{peak}, the energy spectrum of the gamma-ray emission would be such that

$$S(\nu) \propto \begin{cases} \nu^2 & \text{for } h\nu \lesssim E_{\mathrm{peak}}, \\ \nu^{-1} & \text{for } E_{\mathrm{peak}} \lesssim h\nu < \eta h\nu_c. \end{cases} \quad (30)$$

With those estimates, there is a possible synchrotron self-Compton (SSC) generation under some conditions only: in fact, if $r_{\rm acc} > r_b$, the electrons are quickly accelerated beyond 10 GeV, and the SSC process, with keV photons, is in the Klein-Nishina regime ($\bar{\gamma}_e h\nu_{\rm syn} \gg m_e c^2$, where $\bar{\gamma}_e$ is the average Lorentz factor of electrons). Because $\sigma_{\rm KN} \ll \sigma_{\rm T}$, this leads to an associated photospheric radius smaller than $r_{\rm acc}$, so that there is no SSC generation. But if $r_{\rm acc} \simeq r_b$, because of a strong synchrotron energy limitation for electrons, the SSC generation would give rise to very low gamma-ray emission in the GeV range, which would not be observable.

At this stage, it is useful to remark that if we had used a Bohm scaling, the electron energy cutoff due to synchrotron emission would be much higher:

$$\gamma_e^{\rm max} \simeq 3.2\times10^5 \left(\frac{\kappa_0}{10}\right)^{-1/2} \left[\frac{B(r_b)}{10^4\ {\rm G}}\right]^{-1/2} \left(\frac{r}{r_b}\right). \quad (31)$$

This limit, which increases with distance, unlike the Kolmogorov one, would lead to a prohibitively high synchrotron spectrum.

4.2. *Synchrotron Emission by Protons*

Let us first consider the acceleration of protons at internal shocks. The proton acceleration via the usual Fermi acceleration is only limited by the expansion losses, as we have seen in § 3.1. The previous calculation for electrons can be transposed to protons. For protons in the comoving frame, the synchrotron emission is at a maximum at the energy (for $B \propto r^{-2}$)

$$h\nu_{\rm syn} \simeq 1.0\times10^{-6} \left[\frac{B(r_b)}{10^5\ {\rm G}}\right] \left(\frac{r}{r_b}\right)^{-2} \left(\frac{\epsilon}{1\ {\rm GeV}}\right)^2\ {\rm eV}. \quad (32)$$

In the observer frame, the resulting synchrotron spectrum for protons will be such that $S_p(\nu) \propto \nu^{-1}$. According to equation (14), this spectrum extends from 10^{-7} to 1 eV in the comoving frame. These low-energy photons can interact with the accelerated electrons via inverse Compton scattering: in this case, for which $\bar{\gamma}_e h\nu \ll m_e c^2$ with a high average Lorentz factor ($\bar{\gamma}_e \geq 10^3$) of the electrons, the cross section is $\sigma_c \simeq \bar{\gamma}_e^2 \sigma_{\rm T}$. The associated photospheric radius, namely, $r_{\rm ph}$, is such that (see eq. [6]) $r_{\rm ph} \simeq \bar{\gamma}_e r_\star \gg r_b$. During the internal shock phase, the inverse Compton effect thus produces photons with an energy amplified by a factor $\bar{\gamma}_e^2$ and that have an energy spectrum ($\propto \epsilon^{-1/2}$) extending from 0.1 to more than 10^6 eV in the comoving frame, i.e., from 10 eV to 0.1 GeV for the observer.

We consider now UHECRs generated by the additional Fermi process with Lorentz factors, namely, γ in the range [10^8, 10^9] in the comoving frame (Gialis & Pelletier 2004); according to equation (16), the synchrotron energy spectrum will be such that $S_{\rm UHECR}(\nu) \propto \nu^{-1/2}$, and following equation (32), UHECRs radiate synchrotron photons with an energy that scales like r^{-2} because of the decreasing magnetic field. Moreover, for a magnetic field decreasing like r^{-2}, i.e., in the unfavorable conservative assumption, the minimal value at r_b must be $\geq 10^5$ G. According to the acceleration process, we have shown that a sizeable fraction of the UHECR component is achieved around a distance, namely, $r_{\rm cr}$, of a few tens of r_b, typically between $50r_b$ and $100r_b$. Beyond a few $r_{\rm cr}$, the acceleration process is unable to produce UHECRs. However, this generation is efficient enough to get a cosmic-ray pressure that becomes competitive with the magnetic pressure. Actually, the weak point of our description is the absence of a back-reaction of the cosmic-ray pressure on the hydromagnetic fronts, which would deserve a future development. Nevertheless, this acceleration process is more progressive than that based on a Bohm scaling at shocks. This UHECR generation radius, $r_{\rm cr}$, will determine the synchrotron emission range of UHECRs. In fact, because we have

$$\epsilon_{\rm syn}^p = h\nu_{\rm syn}^{\rm UHECR} \simeq 10 \left[\frac{B(r_b)}{10^5\ {\rm G}}\right] \left(\frac{r}{r_b}\right)^{-2} \left(\frac{\gamma}{10^8}\right)^2\ {\rm GeV}, \quad (33)$$

the photons produced by UHECRs may extend from 1 to 400 MeV in the comoving frame.

We have to examine now the consequences of a pair creation process between these hadronic photons and the electronic ones. We have previously seen that the energy of the electronic photons reaches a maximum value of 200 keV at the distance r_c, which can be written as

$$r_c \simeq 148 \left[\frac{B(r_b)}{10^5\ {\rm G}}\right]^{3/4} r_b \quad (34)$$

for $B \propto r^{-2}$ so that we have $r_{\rm cr} < r_c$ if $r_{\rm cr} \simeq 100r_b$. According to the previous results (see § 3.2) and equation (33), the pair creation process happens if the product

$$\epsilon_{\rm syn}^p \epsilon_{\rm syn}^e \simeq 70 \left[\frac{B(r_b)}{10^5\ {\rm G}}\right]^2 \left(\frac{r}{r_b}\right)^{-4} \left(\frac{\epsilon_b}{1\ {\rm MeV}}\right)^2 \left(\frac{\gamma}{10^8}\right)^2\ {\rm keV}^2 \quad (35)$$

is higher than $2(m_e c^2)^2$, i.e., $\simeq 5.2\times10^5$ (keV)^2, where $\epsilon_{\rm syn}^e$ is the energy of electronic photons. The threshold Lorentz factor, $\gamma_{\rm th}$, beyond which the hadronic photons undergo a pair creation can be defined by

$$\gamma_s = \begin{cases} 2.3\times10^8 \left[\dfrac{B(r_b)}{10^5\ {\rm G}}\right]^{1/4} & \text{for } r_{\rm cr} \leq r \leq r_c, \\ 2.3\times10^8 \left[\dfrac{B(r_b)}{10^5\ {\rm G}}\right]^{-2} \left(\dfrac{r}{r_c}\right)^3 & \text{for } r > r_c. \end{cases} \quad (36)$$

Thus, hadronic photons for which the Lorentz factor is between 10^8 and γ_s never undergo the pair creation process; so the corresponding energy for hadronic photons will be in the range $[\epsilon_{\rm syn}^p(\gamma = 10^8), \epsilon_{\rm syn}^p(\gamma_{\rm th})]$ such that

$$\epsilon_{\rm syn}^p(\gamma = 10^8) \simeq 1.0 \left[\frac{B(r_b)}{10^5\ {\rm G}}\right] \left(\frac{r}{r_{\rm cr}}\right)^{-2}\ {\rm MeV} \quad (37)$$

and

$$\epsilon_{\rm syn}^p(\gamma_{\rm th}) \simeq 5.4 \left[\frac{B(r_b)}{10^5\ {\rm G}}\right]^{3/2} \left(\frac{r}{r_{\rm cr}}\right)^{-2}\ {\rm MeV}, \quad (38)$$

with $r_{\rm cr} \simeq 100r_b$ and for $r_{\rm cr} \leq r \leq r_c$. Beyond r_c, the cutoff energy for hadronic photons will be

$$\epsilon_{\rm syn}^p(\gamma_{\rm th}) \simeq 2.5 \left[\frac{B(r_b)}{10^5\ {\rm G}}\right]^{-9/2} \left(\frac{r}{r_c}\right)^4\ {\rm MeV}. \quad (39)$$

Therefore, the previous estimates allow us to predict that an observer can detect synchrotron photons emitted by UHE protons from a few times 0.1 GeV to a few times 10 GeV. We can remark that if $r_{\rm cr} > 225r_b$, then $\epsilon_{\rm syn}^p(\gamma = 10^8) < 200$ keV, and this emission may not be observable because of the electronic

synchrotron component. To end this review of all the possible absorption effects, we note that the interaction of these photons with themselves, which is kinematically possible, leads to a negligible opacity, namely, $\tau_{\gamma\gamma} \sim (E_{\rm syn}/E)\tau_\star \sim (10^{-5}$ to $10^{-4})\tau_\star$.

Let us estimate the corresponding global radiated energy that we compare to the energy in the UHECR component. For an E^{-2} spectrum, assuming a uniform flux during Δt_w, the energy $E_\star$ in the CR component above $\gamma_0 \geq 1$ is

$$E_\star = \Gamma m_p c^3 \Omega r^2 \int_{\gamma_0}^{\gamma_{\rm max}} \rho(\gamma)\gamma\, d\gamma \Delta t_w, \tag{40}$$

where $\rho(\gamma) = n_\star \gamma_0 \gamma^{-2}$ from γ_0 up to $\gamma_{\rm max} \simeq 10^9$ and the number of cosmic rays above γ_0, $N_\star = n_\star(r_b)\Omega r_b^2 c \Delta t_w$. We obtain

$$E_\star = \Gamma m_p c^2 N_\star \gamma_0 \log\left(\frac{\gamma_{\rm max}}{\gamma_0}\right). \tag{41}$$

This can be simply compared to the GRB energy, E, since the total energy injected in protons, $E_p = E_\star(\gamma_0 = 1)$, is a sizeable fraction of E. We can write

$$\frac{E_\star}{E} \sim 1 - \frac{\log \gamma_0}{\log \gamma_{\rm max}}, \tag{42}$$

because $N_p \simeq \gamma_0 N_\star$. Concerning the UHECRs with $\gamma_0 = 10^8$, we find the reasonable result that $E_{\rm UHECR}/E \simeq 10^{-1}$. Let us come back now to the estimate of the radiated energy that could be observed. Beyond the generation radius, $r_{\rm cr}$, each proton synchrotron radiates a total energy

$$e_p^{\rm syn}(\gamma) = \frac{4}{3}\left(\frac{m_e}{m_p}\right)^2 \sigma_{\rm T}\Gamma c \gamma^2 \int_{r_{\rm cr}}^{r_d} \frac{B(r)^2}{8\pi}\, dt, \tag{43}$$

which leads to

$$e_p^{\rm syn}(\gamma) \simeq 9.6\times 10^7 \left(\frac{\eta}{300}\right)^3 \left[\frac{B(r_b)}{10^5\ {\rm G}}\right]^2 \left(\frac{\gamma}{10^8}\right)^2 \left(\frac{r_b}{r_{\rm cr}}\right)^3 \ {\rm ergs}. \tag{44}$$

Thus, because $dN_{\rm UHECR}/d\gamma \simeq 10^8 N_{\rm UHECR}\gamma^{-2} \simeq N_p\gamma^{-2}$, where $N_{\rm UHECR}$ ($\gamma \geq 10^8$) and N_p are, respectively, the total number of UHECRs and protons, the global emission that can be observed will have an energy

$$E_{\rm UHECR}^{\rm syn} \simeq \int_{10^8}^{10^9} N_p e_p^{\rm syn}(\gamma)\gamma^{-2}\, d\gamma, \tag{45}$$

and with $N_p \simeq E/(\eta m_p c^2)$, we obtain

$$\frac{E_{\rm UHECR}^{\rm syn}}{E} \simeq 19\left(\frac{\eta}{300}\right)^2 \left[\frac{B(r_b)}{10^5\ {\rm G}}\right]^2 \left(\frac{r_b}{r_{\rm cr}}\right)^3. \tag{46}$$

For $r_{\rm cr} = (50\text{–}100)r_b$, this ratio is between 10^{-5} and 10^{-4}. This leads to a number of photons of about 10^{-3} to 10^{-5} cm^{-2} for a GRB located at 1 Gpc and pointing toward the observer. But if we consider a slightly higher magnetic field strength of 10^5 G at r_b, this number will increase to around 10^{-3} cm^{-2}. A few GeV photons may be detectable by the *GLAST* instrument, which will have an effective area of about 10^4 cm^2. Finally, this number of detected photons could increase up to about 100 for a GRB located at 100 Mpc.

This will constitute a very interesting signature of the UHECR generation in GRBs and will provide us some constraints on the internal shock model. The only possible competitive emission in that range could be produced by the SSC process at the reverse shock and/or the early external shock under exceptional conditions (Granot & Guetta 2003).

5. CONCLUSION

The combined analysis of both electron and proton acceleration together with the observation data leads to interesting conclusions in the frame of conservative assumptions about the magnetic field and the scattering of particles off its irregularities. Indeed, with a subequipartition magnetic field that decreases like $1/r^2$ but is concentrated in the shells invoked to account for the light curve, we have shown the following points.

1. The low-energy gamma-ray spectrum is satisfactorily explained by the synchrotron radiation of the electrons that are accelerated at the internal shocks with a spectrum displaying the expected peak emission. The lowest energy part of the spectrum would likely be explained by a thermal component. But the connection between both spectra at $E_{\rm peak}$ is not yet clearly understood by us.

2. The possibility of UHECR generation under the previously stated conditions, as proposed in Gialis & Pelletier (2004), is confirmed, and the estimated flux is in agreement with the expected one (Waxman 1995) that accounts for the cosmic-ray spectrum around the ankle. A detailed estimate of the GRB contribution of the UHECRs to the cosmic-ray spectrum, which is currently recorded by the Pierre Auger Observatory, has been proposed by Bahcall & Waxman (2001); it displays the expected excess around the GZK threshold.

3. The generation of cosmic rays in GRBs often starts before the fireball becomes transparent to *pp* collisions. This gives rise to a gamma-ray emission around 20 GeV due to π^0 decay. This emission is not contaminated by the SSC emission of the electrons, because that latter emission is in the Klein-Nishina regime. We can also expect that neutrons are produced by these *pp* collisions; they decay after some travel and thus generate a significant neutrino flux of 200 MeV (observer frame).

4. The most plausible signature of UHECR generation is not related to the $p\gamma$ process but more likely to their synchrotron emission. Indeed, the ratio of the corresponding luminosities $L_{p\gamma}/L_{\rm syn} \simeq U_s/U_{\rm mag}$, where U_s is the energy density of the soft photons and $U_{\rm mag}$ is the energy density of the magnetic field, turns out to be on the order of unity. Since the energy of the neutrinos ($\sim$TeV for the observer) emitted through the $p\gamma$ process is much higher than the energy of the gamma-ray photons ($\sim$GeV) emitted by the synchrotron process, the neutrinos are 1000 times less numerous than the photons. Thanks to our conservative assumption about the magnetic field, a gamma-ray flux can be so emitted and could be observed. Indeed, we found a natural range of gamma-ray energies for which the fireball is transparent to the pair creation process, because of the chronology of the emissions during the fireball expansion and the magnetic field decreases as r^{-2}. This range typically extends from a few hundred MeV to 10 GeV. It turns out that the observation of GeV photons should be a signature of UHECRs with probably no confusion. This could be observed by *GLAST*. At 1 Gpc, a 10^5 G field would lead to a significant number of events, which, of course, increases at shorter distances. This would be a very interesting signature of UHECR generation in GRBs.

APPENDIX

We detail the exact determination of the synchrotron spectrum as defined by equation (28). Let us rewrite this expression as

$$S_e(\nu) \propto \nu^{-1/2}\left[\int_{r_b}^{r_c} \frac{1}{r^3}\exp\left(-\alpha\frac{r_c}{r}\right)dr + \int_{r_c}^{r_d}\frac{1}{r^3}\exp\left(-\alpha\frac{r^2}{r_c^2}\right)dr\right], \tag{A1}$$

where $\alpha \equiv (\nu/\nu_c)^{1/2} \geq [\nu_{\rm syn}(r_b)/\nu_c]^{1/2} \simeq 3.9\times10^{-2}$.

First, a simple integration by parts leads to

$$\int_{r_b}^{r_c}\frac{1}{r^3}\exp\left(-\alpha\frac{r_c}{r}\right)dr = \frac{1}{r_c^2\alpha^2}\left[(\alpha+1)\exp(-\alpha) - \frac{\alpha+\lambda}{\lambda}\exp\left(-\frac{\alpha}{\lambda}\right)\right], \tag{A2}$$

with $\lambda = r_b/r_c \simeq 1/26$ for $B \propto r^{-2}$.

For the second integral, because $r_c \ll r_d$, we can assume $r_d \rightarrow +\infty$, and after a first integration by parts, we can write, for instance,

$$\int_{r_c}^{r_d}\frac{1}{r^3}\exp\left(-\alpha\frac{r^2}{r_c^2}\right)dr = \frac{r_c^2}{2\alpha}\left[\frac{\exp(-\alpha)}{r_c^4} - 4\int_{r_c}^{+\infty}\frac{1}{r^5}\exp\left(-\alpha\frac{r^2}{r_c^2}\right)dr\right]. \tag{A3}$$

An iterative integration by parts gives, with some manipulations, the following result:

$$\int_{r_c}^{r_d}\frac{1}{r^3}\exp\left(-\alpha\frac{r^2}{r_c^2}\right)dr = \frac{\exp(-\alpha)}{2r_c^2\alpha}\left(\sum_{n=0}^{+\infty}\frac{(-1)^n(n+1)!}{\alpha^n}\right), \tag{A4}$$

where the sum of the series is convergent for any α according to the generalized hypergeometric function (or Barnes's extended hypergeometric function). For $\alpha = \alpha_{\rm min} \simeq 3.9\times10^{-2}$, this sum is equal to 3.5×10^{-2}, and for $\alpha = 1$, the sum reaches 0.4.

Thus, the synchrotron spectrum $S_e(\nu)$ is such that

$$S_e(\nu) \propto \nu^{-1}\left\{\left[\frac{\alpha+1}{\alpha} + \frac{1}{2}\sum_{n=0}^{+\infty}\frac{(-1)^n(n+1)!}{\alpha^n}\right]\exp(-\alpha) - \frac{\alpha+\lambda}{\lambda\alpha}\exp(-\alpha/\lambda)\right\}. \tag{A5}$$

For $\alpha_{\rm min} \leq \alpha < 1$, the expression between brackets is quasi-constant so that $S_e(\nu) \propto \nu^{-1}$. Beyond $\alpha = 1$, the same expression leads to a spectrum decreasing like ν^{-s} with $s \in [1.5, 2]$.

REFERENCES

Bahcall, J., & Waxman, E. 2001, Phys. Rev. D, 64, 023002
Band, D., et al. 1993, ApJ, 413, 281
Cassé, F., Lemoine, M., & Pelletier, G. 2001, Phys. Rev. D, 65, 3002
Daigne, F., & Mochkovitch, R. 1998, MNRAS, 296, 275
Frail, D. A., et al. 2001, ApJ, 562, L55
Ghirlanda, G., Celotti, A., & Ghisellini, G. 2003, A&A, 406, 879
Gialis, D., & Pelletier, G. 2003, Astropart. Phys., 20, 323
———. 2004, A&A, 425, 395
Goldreich, P., & Shridar, S. 1995, ApJ, 438, 763
Goodman, J. 1986, ApJ, 308, L47
Granot, J., & Guetta, D. 2003, ApJ, 598, L11
Lemoine, M. 2003, in SF2A-2003: Semaine de l'Astrophysique Francaise, ed. F. Combes et al. (Paris: Editions de Physique), 429
Mészáros, P., Laguna, P., & Rees, M. J. 1993, ApJ, 415, 181
Rees, M. J., & Mészáros, P. 1992, MNRAS, 258, 41P
———. 1994, ApJ, 430, L93
Sigl, G., Lemoine, M., & Biermann, P. 1999, Astropart. Phys., 10, 141
van Putten, M. H. P. M., & Regimbau, T. 2003, ApJ, 593, L15
Waxman, E. 1995, Phys. Rev. Lett., 75, 386